JOURNAL OF THE AMERICAN CHEMICAL SOCIETY

Subscriber access provided by ISTANBUL TEKNIK UNIV

Article

Highly Stable Organic Monolayers for Reacting Silicon with Further Functionalities: The Effect of the C#C Bond nearest the Silicon Surface

Sreenivasa Reddy Puniredd, Ossama Assad, and Hossam Haick

J. Am. Chem. Soc., **2008**, 130 (41), 13727-13734 • DOI: 10.1021/ja804674z • Publication Date (Web): 20 September 2008

Downloaded from http://pubs.acs.org on February 8, 2009

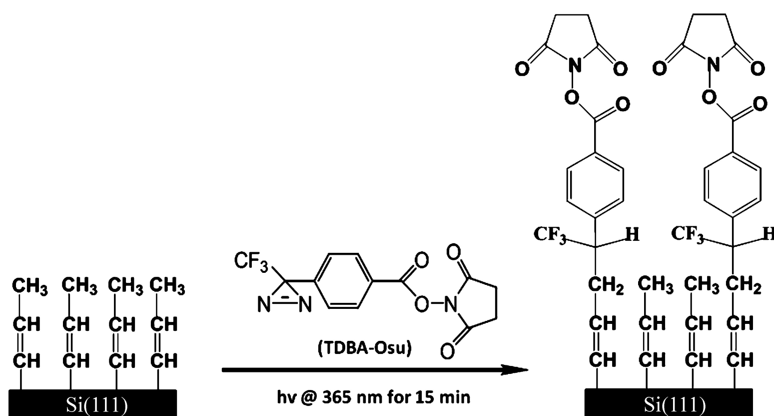

More About This Article

Additional resources and features associated with this article are available within the HTML version:

- Supporting Information
- Links to the 2 articles that cite this article, as of the time of this article download
- Access to high resolution figures
- Links to articles and content related to this article
- Copyright permission to reproduce figures and/or text from this article

View the Full Text HTML

ACS Publications
High quality. High impact.

Journal of the American Chemical Society is published by the American Chemical Society. 1155 Sixteenth Street N.W., Washington, DC 20036

J|A|C|S
ARTICLES
Published on Web 09/20/2008

Highly Stable Organic Monolayers for Reacting Silicon with Further Functionalities: The Effect of the C−C Bond nearest the Silicon Surface

Sreenivasa Reddy Puniredd, Ossama Assad, and Hossam Haick*

The Department of Chemical Engineering and Russell Berrie Nanotechnology Institute, Technion−Israel Institute of Technology, Haifa 32000, Israel

Received June 19, 2008; E-mail: hhossam@technion.ac.il

Abstract: Crystalline Si(111) surfaces have been alkylated in a two-step chlorination/alkylation process using various organic molecules having similar backbones but differing in their C−C bond closest to the silicon surface (i.e., C−C vs C═C vs C≡C bonds). X-ray photoelectron spectroscopic (XPS) data show that functionalization of silicon surfaces with propenyl magnesium bromide (CH_3−CH═CH−MgBr) organic molecules gives nearly full coverage of the silicon atop sites, as on methyl- and propynyl-terminated silicon surfaces. Propenyl-terminated silicon surface shows less surface oxidation and is more robust against solvent attacks when compared to methyl- and propynyl-terminated silicon surfaces. We also show a secondary functionalization process of propenyl-terminated silicon surface with 4′-[3-Trifluoromethyl-3H-diazirin-3-yl]-benzoic acid *N*-hydroxysuccinimide ester [TDBA-OSu] cross-linker. The Si−CH═CH−CH_3 surfaces thus offer a means of attaching a variety of chemical moieties to a silicon surface through a short linking group, enabling applications in molecular electronics, energy conversion, catalysis, and sensing.

1. Introduction

Densely packed organic layers bonded covalently to crystalline silicon (Si) surfaces without an interfacial silicon oxide (SiO_2) layer have received an increasing interest, mainly because of their variety of applications in micro- and nanoelectronics[1−8] as well as in (bio)chemical sensors.[9−16] Attachment of organic species on a Si substrate without intervening oxide could significantly reduce the density of trap states on Si surfaces.[17−19] Furthermore, it might potentially prevent diffusion of oxygen atoms into the monolayer/Si interface during either growth of insulating layer or postannealing process in the formation of high-dielectrics on Si.[20,21]

A variety of surface passivation methods have been investigated to preserve the nearly ideal electrical properties of the H-terminated Si(111) surfaces in ambient conditions.[22−24] The formation of Si−C bonds, however, has attracted a particular interest due to the kinetic inertness of these bonds as compared to Si−O or Si−H bonds. The Si−C bond is chemically more stable than Si−O bonds on oxidized Si surfaces and thus less susceptible to nucleophilic substitution reactions.[25] Si(111) surfaces have been functionalized by a variety of methods, including reaction with alkenes through a radical process catalyzed by a diacyl peroxide initiator,[26,27] use of UV[28−30] or

* To whom correspondence should be addressed. Phone: +972-4-8293087. Fax: +972-4-8295672.

(1) Barrelet, C. J.; Robinson, D. B.; Cheng, J.; Hunt, T. P.; Quate, C. F.; Chidsey, C. E. D. *Langmuir* **2001**, *17*, 3460–3465.
(2) Cheng, J.; Robinson, D. B.; Cicero, R. L.; Eberspacher, T.; Barrelet, C. J.; Chidsey, C. E. D. *J. Phys. Chem. B* **2001**, *105*, 10900–10904.
(3) Buriak, J. M. *Chem. Commun.* **1999**, 1051–1060.
(4) Wolkow, R. A. *Annu. Rev. Phys. Chem.* **1999**, *50*, 413–441.
(5) Cicero, R. L.; Linford, M. R.; Chidsey, C. E. D. *Langmuir* **2000**, *16*, 5688–5695.
(6) Terry, J.; Linford, M. R.; Wigren, C.; Cao, R. Y.; Pianetta, P.; Chidsey, C. E. D. *J. Appl. Phys.* **1999**, *85*, 213–221.
(7) Yamada, T.; Takano, N.; Yamada, K.; Yoshitomi, S.; Inoue, T.; Osaka, T. *J. Electroanal. Chem.* **2002**, *532*, 245–250.
(8) Yamada, T.; Inoue, T.; Yamada, K.; Takano, N.; Osaka, T.; Harada, H.; K. Nishiyama, K.; Taniguchi, I. *J. Am. Chem. Soc.* **2003**, *125*, 8039–8042.
(9) Yates, J. T., Jr. *Science* **1998**, *279*, 335–336.
(10) Wayner, D. D. M.; Wolkow, R. A. *J. Chem. Soc., Perkin Trans.* **2002**, *2*, 23–34.
(11) Buriak, J. M. *Chem. Rev.* **2002**, *102*, 1271–1308.
(12) Boukherroub, R.; Morin, S.; Wayner, D. D. M.; Bensebaa, F. G.; Sproule, I. J.; Baribeau, M.; Lockwood, D. J. *Chem. Mater.* **2001**, *13*, 2002–2011.
(13) Wojtyk, J. T. C.; Tomietto, M.; Boukherroub, R.; Wayner, D. D. M. *J. Am. Chem. Soc.* **2001**, *123*, 1535–1536.
(14) Bent, S. F. *J. Phys. Chem. B* **2002**, *106*, 2830–2842.
(15) Lasseter, T. L.; Clare, B. H.; Abbott, N. L.; Hamers, R. J. *J. Am. Chem. Soc.* **2004**, *126*, 10220–10221.
(16) Zhang, G.-J.; Chua, J. H.; Chee, R.-E.; Agarwal, A.; Wong, S. M.; Buddharaju, K. D.; Balasubramanian, N. *Biosens. Bioelectron* **2008**, *23*, 1701–1707.
(17) Webb, L. J.; Michalak, D. J.; Biteen, J. S.; Brunschwing, B. S.; Chan, A. S. Y.; Knapp, D. W.; Meyer, H. M.; Nemanick, E. J.; Traub, M. C.; Lewis, N. S. *J. Phys. Chem. B.* **2006**, *110*, 23450–23459.
(18) Buczkowski, A.; Radzimski, Z. J.; Rozgonyi, G. A.; Shimura, F. J. *Appl. Phys. Lett.* **1991**, *69*, 6495–6499.
(19) Liu, Y.-J.; Yu, H.-Z. *ChemPhysChem* **2002**, *3*, 799–802.
(20) Higashi, G. S.; Chabal, Y. J.; Trucks, G. W.; Raghavachari, K. *Appl. Phys. Lett.* **1990**, *56*, 656–658.
(21) Liu, Y.-J.; Yu, H.-Z. *J. Phys. Chem. B* **2003**, *107*, 7803–7811.
(22) Liu, Y.-J.; Yu, H.-Z. *ChemPhysChem* **2003**, *4*, 335–342.
(23) Chabal, Y.; Feldman, L. C. *Interface* **2005**, *14*, 31–40.
(24) Miramond, C.; Vuillaume, D. *J. Appl. Phys.* **2004**, *96*, 1529–1536.
(25) Faber, E. J.; de Smet, L. C. P. M.; Olthuis, W.; Zuilhof, H.; Sudhoelter, E. J. R.; Bergveld, P.; van den Berg, A. *ChemPhysChem* **2005**, *6*, 2153–2166.
(26) Linford, M. R.; Chidsey, C. E. D. *J. Am. Chem. Soc.* **1993**, *115*, 12631–12632.
(27) Linford, M. R.; Fenter, P.; Eisenberger, P. M.; Chidsey, C. E. D. *J. Am. Chem. Soc.* **1995**, *117*, 3145–3155.

white[31] light, thermal energy,[32,33] transition-metal complexes,[34] Lewis acid catalysts,[35−37] electrochemical functionalization,[38,39] radical halogenation,[40] and chemomechanical scribing.[41−43] However, these reactions may lead to significant amounts of oxygen on the surface unless extraordinary measures are taken.[44] This unwanted oxidation reaction is the likely source of electrically active defects observed in electrical measurements of arrays of metal−insulator−semiconductor diodes,[25,45−47] including cases where low levels of oxide are not detectable via surface analysis techniques (e.g., XPS or FTIR).[48]

Whatever the maximum number of Si−C bonds, it is clear that a significant number of unreacted Si−H sites still remain on the surface. Consequently, the surfaces are vulnerable to oxidation by water and oxygen, which can penetrate through the monolayer. This inherent instability is inconsistent with the development of stable, robust sensors—the application cited by most of the published works in this area.[49,50] The problem is that oxidation of silicon can result in the formation of electrically active surface states that change the electrical properties of the underlying silicon.[25,51,52] Any strategy that aims toward hybrid silicon−organic devices should ideally limit the number of oxide-based surface states and, at minimum, stabilize them so they do not change over time.[50]

Fresh Si surfaces alkylated via two step chlorination/alkylation (Grignard reagent) with straight-chain alkyl groups (C_nH_{2n+1}, $n = 1-8$)[40,52] have shown surface passivation both chemically and electrically.[52−54] The passivation properties, however, degraded partially within a few weeks of exposure to ambient conditions and within shorter periods upon exposure to water and/or other organic solvents.[26,49−57] If their stability properties are excluded, the structurally simple alkyl monolayers directly bonded to silicon surfaces can be useful as high-resolution lithography materials in the next generation of nanofabrications.

Complete coverage of Si atop sites was achieved by CH_3 termination of Si(111) through a two-step chlorination/alkylation process.[52,58] Though CH_3 termination gives ~100% coverage, further functionalization (by reaction with other molecules) is not possible. To compensate for this limitation of CH_3−Si surfaces, Si(111) surfaces have been terminated with acetylenic functionality via Si−C bonding.[59] The obtained coverage of these molecules was identical to that of the CH_3-terminated Si(111) surface, viz., full termination of the Si atop sites on an unreconstructed Si(111) surface. In contrast to CH_3 groups attached to Si surfaces, the acetylene molecules provided a reactive functionality for further chemical modification of the Si surfaces.[59] Surfaces terminated with acetylenic functionality, though, oxidize after a certain period of time (see ref 59, Figure 1C, and Figure 2).

We report herein an approach to protect silicon surfaces with CH_3−CH═CH−MgBr organic molecules using a two-step chlorination/Grignard process. We compare the properties of this film with various organic molecules having similar backbones but differing in their C−C bond closest to the Si surface (i.e., C−C vs C═C vs C≡C bonds). We show that functionalization of Si surfaces with CH_3−CH═CH−MgBr organic molecules gives nearly full coverage of the Si atop sites. Further, we have studied the surface oxidation and solvent attacks against these molecules attached to silicon surfaces. Finally, we describe a functionalization process of propenyl-terminated surfaces with TDBA-OSu cross-linker that also provides a scaffold for further facile functionalization of the Si surface. A preliminary report has appeared in the literature.[60]

2. Experimental Section

2.1. Materials. Silicon wafers were (111)-oriented, single-side polished, 525 ± 25 μm thick, n-type, Sb-doped samples, with a resistivity of 0.008−0.020 Ω cm (Virginia Semiconductor Inc.). Except as noted, all reagents used were ACS reagent grade, were stored in a nitrogen-purged glovebox, and were used as received. Water rinses used 18 MΩ cm resistivity deionized (DI) water obtained from a Millipore Nanopure system.

Methanol, acetone, hexane, dichloromethane, 1,1,1-trichloroethane (all from Frutarom Ltd.), anhydrous tetrahydrofuran (THF)

(28) Terry, J.; Linford, M. R.; Wigren, C.; Cao, R. Y.; Pianetta, P.; Chidsey, C. E. D. *Appl. Phys. Lett.* **1997**, *71*, 1056–1058.
(29) Terry, J.; Mo, R.; Wigren, C.; Cao, R. Y.; Mount, G.; Pianetta, P.; Linford, M. R.; Chidsey, C. E. D. *Nucl. Instrum. Methods B* **1997**, *133*, 94–101.
(30) Effenberger, F.; Gotz, G.; Bidlingmaier, B.; Wezstein, M. *Angew. Chem., Int. Ed.* **1998**, *37*, 2462–2464.
(31) Stewart, M. P.; Buriak, J. M. *Angew. Chem., Int. Ed.* **1998**, *23*, 3257–3260.
(32) Sieval, A. B.; Demirel, A. L.; Nissink, J. W. M.; Linford, M. R.; van der Maas, J. H.; de Jeu, W. H.; Zuilhof, H.; Sudholter, E. J. R. *Langmuir* **1998**, *14*, 1759–1768.
(33) Sung, M. M.; Kluth, G. J.; Yauw, O. W.; Maboudian, R. *Langmuir* **1997**, *13*, 6164–6168.
(34) Zazzera, L. A.; Evans, J. F.; Deruelle, M.; Tirrell, M.; Kessel, C. R.; Mckeown, P. *J. Electrochem. Soc.* **1997**, *144*, 2184–2189.
(35) Buriak, J. M.; Allen, M. J. *J. Am. Chem. Soc.* **1998**, *120*, 1339–1340.
(36) Buriak, J. M.; Allen, M. J. *J. Lumin.* **1998**, *80*, 29–35.
(37) Holland, J. M.; Stewart, M. P.; Allen, M. J.; Buriak, J. M. *J. Solid State Chem.* **1999**, *147*, 251–258.
(38) Henry de Villeneuve, C.; Pinson, J.; Ozanam, F.; Chazalviel, J. N.; Allongue, P. *Mater. Res. Soc. Symp. Proc.* **1997**, *451*, 185–195.
(39) Vieillard, C.; Warntjes, M.; Ozanam, F.; Chazalviel, J.-N. *Proc. Electrochem. Soc.* **1996**, *95*, 250–258.
(40) Bansal, A.; Li, X.; Lauermann, I.; Lewis, N. S.; Yi, S. I.; Weinberg, W. H. *J. Am. Chem. Soc.* **1996**, *118*, 7225–7226.
(41) Niederhauser, T. L.; Jiang, G.; Lua, Y.-Y.; Dorff, M. J.; Woolley, A. T.; Asplund, M. C.; Berges, D. A.; Linford, M. R. *Langmuir* **2001**, *19*, 5889–5900.
(42) Niederhauser, T. L.; Lua, Y.-Y.; Sun, Y.; Jiang, G.; Strossman, G. S.; Pianetta, P.; Linford, M. R. *Chem. Mater.* **2002**, *14*, 27–29.
(43) Niederhauser, T. L.; Lua, Y.-Y.; Jiang, G.; Davis, S. D.; Matheson, R.; Hess, D. A.; Mowat, I. A.; Linford, M. R. *Angew. Chem., Int. Ed.* **2002**, *41*, 2353–2356.
(44) Hart, B. R.; Letant, S. E.; Kane, S. R.; Hadi, M. Z.; Shields, S. J.; Reynolds, J. G. *Chem. Commun.* **2003**, 322–323.
(45) Sieval, A. B.; Vleeming, V.; Zuilhof, H.; Sudhölter, E. J. R. *Langmuir* **1999**, *15*, 8288–8291.
(46) Salomon, A.; Böcking, T.; Gooding, J. J.; Cahen, D. *Nano Lett.* **2006**, *6*, 2873–2876.
(47) Yu, H. Z.; Boukherroub, R.; Morin, S.; Wayner, D. D. M. *Electrochem. Commun.* **2000**, *2*, 562–566.
(48) Seitz, O.; Böcking, T.; Salomon, A.; Gooding, J. J.; Cahen, D. *Langmuir* **2006**, *22*, 6915–6922.
(49) Gorostiza, P.; Henry de Villeneuve, C.; Sun, Q. Y.; Sanz, F.; Wallart, X.; Boukherroub, R.; Allongue, P. *J. Phys. Chem. B* **2006**, *110*, 5576–5581.
(50) Bin, X.; Mischki, T. K.; Fan, C.; Lopinski, G. P.; Wayner, D. D. M. *J. Phys. Chem. C* **2007**, *111*, 13547–13553.
(51) Rivillon, S.; Chabal, Y. J. *J. Phys. IV France* **2006**, *132*, 195–200.
(52) Webb, L. J.; Lewis, N. S. *J. Phys. Chem. B* **2003**, *107*, 5404–5412.
(53) Bansal, A.; Li, X. L.; Yi, S. I.; Weinberg, W. H.; Lewis, N. S. *J. Phys. Chem. B* **2001**, *105*, 10266–10277.
(54) Royea, W. J.; Juang, A.; Lewis, N. S. *Appl. Phys. Lett.* **2000**, *77*, 1988–1990.
(55) Bansal, A.; Lewis, N. S. *J. Phys. Chem. B* **1998**, *102*, 1067–1070.
(56) Bansal, A.; Lewis, N. S. *J. Phys. Chem. B* **1998**, *102*, 4058–4060.
(57) Yu, H.; Webb, L. J.; Ries, R. S.; Solares, S. D.; Goddard, W. A., III; Heath, J. R.; Lewis, N. S. *J. Phys. Chem. B* **2005**, *109*, 671–674.
(58) Nemanick, E. J.; Hurley, P. T.; Brunschwig, B. S.; Lewis, N. S. *J. Phys. Chem. B* **2006**, *110*, 14800–14808.
(59) Hurley, P. T.; Nemanick, E. J.; Brunschwig, B. S.; Lewis, N. S. *J. Am. Chem. Soc.* **2006**, *128*, 9990–99901.
(60) Puniredd, S. R.; Assad, O.; Haick, H. *J. Am. Chem. Soc.* **2008**, *130*, 9184–9185.

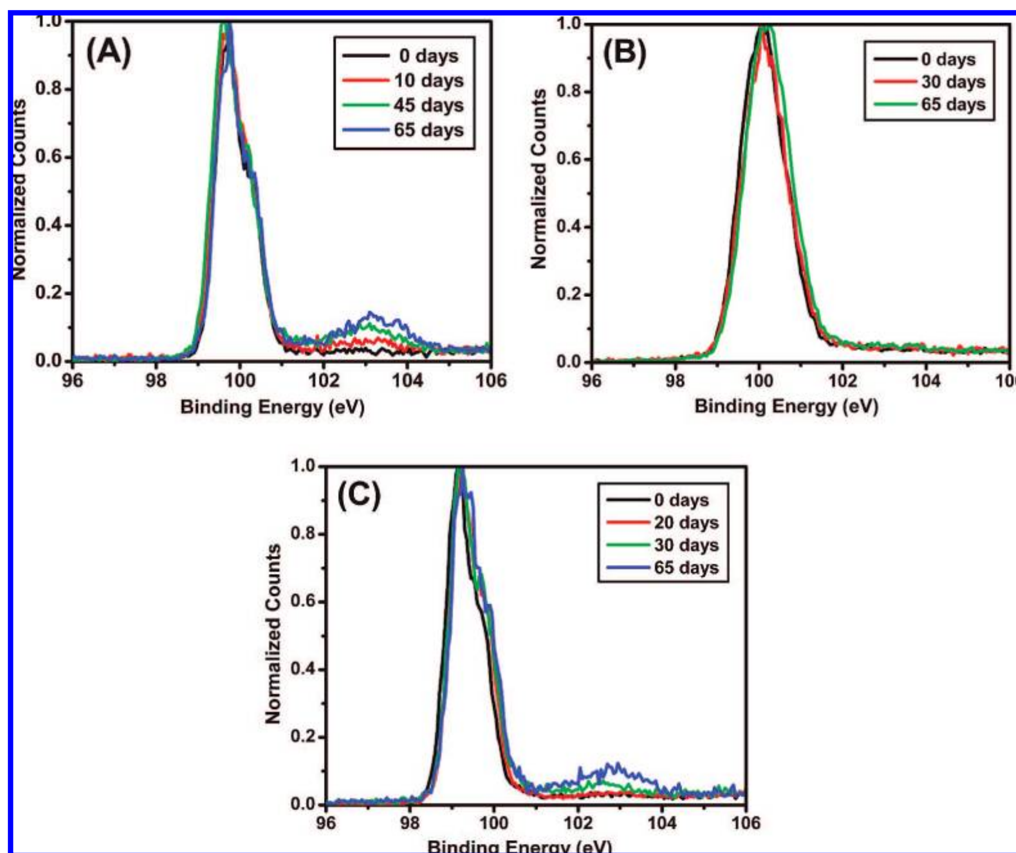

Figure 1. XPS data showing the oxidation in the Si2p region for (A) Si−CH_3 after 0, 10, 45, and 65 days in air; (B) Si−CH═CH−CH_3 at 0, 30, and 65 days in air; and (C) Si−C≡C−CH_3 at 0, 20, 30, and 65 days in air.

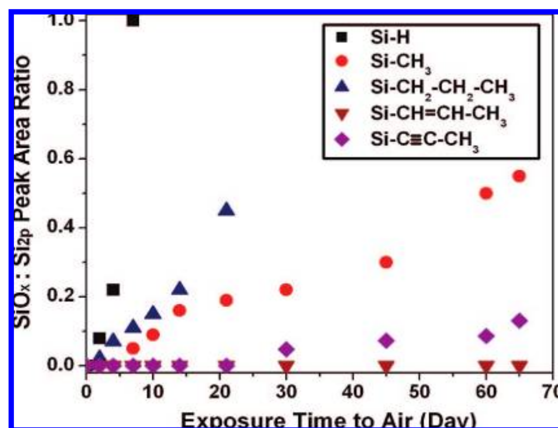

Figure 2. Oxidation (SiOx/Si2p peak-area ratio) of molecularly modified Si(111) surfaces versus exposure time to ambient conditions in the dark.

and chlorobenzene (both from Sigma-Aldrich), phosphorus pentachloride (PCl_5), benzoyl peroxide (97%, Sigma-Aldrich), anhydrous carbon tetrachloride (Merck), and 4′-[3-trifluoromethyl-3*H*-diazirin-3-yl]-benzoic acid *N*-hydroxysuccinimide ester [TDBA-OSu] (Toronto Research Chemicals Inc., Canada) were used as received. A 3.0 M solution of methylmagnesium chloride (CH_3MgCl) in THF, a 0.5 M solution of 1-propenylmagnesium bromide (CH_3−CH═CH−MgBr) in THF, a 0.5 M solution of 1-propynylmagnesium bromide (CH_3−C≡C−MgBr) in THF, and a 2.0 M solution of propylmagnesium chloride (CH_3−CH_2−CH_2−MgCl) in diethyl ether were used as received.

2.2. Sample Preparation and Functionalization. Prior to chemical modification, all Si(111) surfaces were cleaned by sequential rinsing with DI water, methanol, acetone, dichloromethane, 1,1,1-trichloroethane, acetone, methanol, and DI water. Samples were then dried under a stream of N_2(g). H-terminated Si(111) surfaces were obtained through wet chemical etching for 20 min in 40% NH_4F(aq) (Sigma-Aldrich). The samples were agitated periodically to minimize the formation of etch pits. Following etching, the monohydride-terminated surfaces were rinsed by flowing DI water and dried under a stream of N_2(g). Si−H samples were alkylated using the two-step chlorination/alkylation protocol.[52,53] A freshly etched surface was first immersed in a saturated solution of PCl_5 (99.998%, Alfa Aesar) in chlorobenzene to which a few grains of benzoyl peroxide had been added. The reaction solution was then heated to 90−100 °C for 45 min. The chlorinated samples were rinsed sequentially with chlorobenzene and THF, and the samples were transferred to a N_2-purged glovebox. The samples were subsequently immersed for 27 h at 120−130 °C in 0.5 M THF solutions of CH_3−CH═CH−MgBr and CH_3−C≡C−MgBr for producing Si−CH═CH−CH_3 and Si−C≡C−CH_3 surfaces, respectively. A 20 h immersion in a 2.0 M diethyl ether solution of CH_3−CH_2−CH_2−MgCl was used to produce the Si−CH_2−CH_2−CH_3 surface. A 10 h immersion in a 3.0 M THF solution of CH_3MgCl was used for producing the CH_3-terminated Si surface (Si−CH_3).[58] Alkylated Si samples were rinsed with flowing THF and then immersed in methanol. The alkylated samples were transported out of the glovebox and further rinsed with methanol, sonicated in fresh methanol and 1,1,1-trichloroethane, rinsed with H_2O, and dried under a stream of N_2(g).

2.3. Secondary Functionalization of Propenyl-Terminated Si(111) Surface. Silicon (111) wafer pieces with propenyl monolayers were placed in a 10 mm quartz cuvette with the polished side pointing upward. Then, 0.2 mL of a 15 mM solution of TDBA-OSu in dry carbon tetrachloride was added and immediately illuminated with a broadband 365 nm UV lamp at a distance of 4

cm for 15 min. The samples were then rinsed vigorously with carbon tetrachloride, CH_2Cl_2, and water.[61]

2.4. Instrumentation. 2.4.1. X-ray Photoelectron Spectroscopy (XPS). Surface analysis of films was performed by XPS, using a Thermo VG Scientific, Sigma probe, England, having a base pressure of $<3 \times 10^{-9}$ Torr and fitted with a monochromatized Al Kα (1486.6 eV) X-ray source. The measurements were performed in the surface and bulk-sensitive modes at a takeoff angle, θ, between the direction of an analyzer and the specimen plane of 14.5° and 59.5°, respectively. All measurements were taken on the center of the sample to ensure reproducibility and to minimize the effects of scratches or contamination at the edges. Samples were first scanned from 0 to 1000 binding eV to monitor signals for carbon and oxygen. The Si2p and C1s regions of 98−105 and 282−287 eV, respectively, were investigated in detail. The Si2p region was used to monitor the growth of Si oxides. Spectral analysis was performed using the peak fitting software (*XPSPEAK* version 4.1) after a Shirley background subtraction. For Si2p data analysis, the spectra were first fit to a Shirley background, which was then subtracted to allow for peak fitting. The position of the $Si2p_{1/2}$ peak was fixed at a binding energy 0.6 eV higher than that of the $Si2p_{3/2}$ peak, and the full width at half maximum of the $Si2p_{1/2}$ peak was constrained to be identical to that of the $Si2p_{3/2}$ peak, with the $2p_{1/2}/2p_{3/2}$ total integrated peak-area ratio fixed at 0.51.[58]

Three functions were used, representing silicon-bonded carbon at 284.0 eV, carbon-bonded carbon at 285.2 eV, and oxygen-bonded carbon at 286.6 eV.[52,57,58] The peak centers were allowed to float, though the center-to-center distances were fixed at 1.2 eV between the silicon-bonded carbon and carbon-bonded carbon emissions and at 1.6 eV between the oxygen-bonded carbon and carbon-bonded carbon emissions. The integrated area under each carbon peak was ratioed to the integrated area under the Si2p peaks for that sample and normalized for scan time. The ratio of the silicon-bonded carbon (i.e., C−Si) to the normalized area for the Si2p peak, C−Si/Si2p, was then compared between alkylated surfaces. Surface coverages for each alkyl group are reported relative to the value of C−Si/Si2p observed for CH_3-terminated Si(111) surfaces.[57,58]

2.4.2. Time-of-Flight Secondary Ion Mass Spectroscopy (ToF-SIMS) Analysis. The spectra were recorded with a ToF.-SIMS5 system (ION-TOF GmbH) in the positive and negative modes. A 25 keV, 1pA, 209 Bi^{1+} pulsed primary beam was rastered over a 500 × 500 μm^2 area, and the total primary ion dose was kept well below the static limit (<1012 ions cm^{-2}). No charge compensation was required. The mass resolution for the characteristic fragments studied ($SiCH_3^+$, $SiC_3H_3^+$, $SiC_3H_5^+$, $SiC_3H_7^+$, CH_3^-, $C_3H_3^-$, $C_3H_5^-$, $C_3H_7^-$, and SiO_2) was above 9000. The normalization to the spectrum total ion intensity was added for both positive and negative modes.

2.4.3. Spectroscopic Ellipsometery. Ellipsometric spectra were recorded over a range from 250 to 1000 nm at three different incidence angles, 65, 70, and 75°, using a spectroscopic phase-modulated ellipsometer (M-2000V Automated Angle, J. A. Woollam Co., Inc., USA). The modeling for the thin-film measurement used (Si.MAT) as the base layer with 0.5 mm thickness and the Cauchy package (CAUCHY MAT) for the film material. The bare reference (Si−H) sample was used as a reference sample. We used a three-phase air/monolayer/substrate model to extract the thickness of the monolayer. Taking multiple readings and using the average value of the most consistent readings minimized errors in the thickness measurements.

2.5. Quantum-Mechanical Calculations. Density functional theory (DFT) calculations using the GO3W package with the B3LYP method and a 6-311G basis set were used to calculate the lengths of the free molecules studied here.

(61) Wagner, P.; Nock, S.; Spudich, J. A.; Volkmuth, W. D.; Chu, S.; Cicero, R. L.; Wade, C. P.; Linford, M. R.; Chidsey, C. E. D. *J. Struct. Biol.* **1997**, *119*, 189–201.

Table 1. C−Si/Si2p XPS Integrated Peak-Area Ratios for Alkylated Si(111) Surfaces Showing the Relative Amount of Carbon Bonded to Silicon for Each Alkylated Surface

	C−Si/Si2p ratio	% of methyl coverage
methyl ($Si-CH_3$)	0.160 ± 0.02	
propyl ($Si-CH_2-CH_2-CH_3$)	0.071 ± 0.02	50 ± 10
propenyl ($Si-CH=CH-CH_3$)	0.175 ± 0.01	110 ± 10
propynyl ($Si-C\equiv C-CH_3$)	0.165 ± 0.01	105 ± 05

3. Results and Discussion

3.1. XPS Analysis. Two main emissions at 284.0 and 285.2 eV and a third signal at 286.6 eV were observed for methyl- (CH_3-), propyl- ($CH_3-CH_2-CH_2-$), propenyl- ($CH_3-CH=CH-$), and propynyl- ($CH_3-C\equiv C-$) terminated Si(111) surfaces. The emissions located at 285.2 and 286.6 eV were also observed for H-terminated Si(111) surfaces, whereas the low binding energy emission at 284.0 eV was unique to alkylated Si surfaces.[28,58−60] Hence, the first peak at 284.0 eV can be assigned to emission from core-level electrons of carbon atoms covalently bonded to the relatively electropositive silicon (C−Si).[52,57−60] The second C1s peak, characterized by an energy emission at 285.2 eV, can be ascribed to carbon bonded to either hydrogen or another carbon atom. The third C1s peak, characterized by a binding energy at 286.6 eV, is ascribed to adventitious carbon bonded to oxygen from the wet chemical processing with THF solvent and THF/methanol rinse after functionalization, from carbonaceous materials present in the laboratory environment, and/or from the transportation of samples to the XPS chamber. The two peaks at higher energy (i.e., 285.0 and 286.6 eV) may also contain contributions from vibrational excitations associated with lower-energy peaks.[28,52,59,60] The Si2p spectrum shows $Si2p_{3/2}$ and $Si2p_{1/2}$ with the expected 2:1 area ratio and 0.6 eV energy separation observed for methyl-, propyl-, propenyl-, and propynyl-terminated Si(111) surfaces. No oxidized Si between 101.0 and 103.5 eV was observed, confirming the absence of SiO_2 after alkylation.[52,57−59]

The C1s peak at 284.0 eV (C−Si) provides semiquantitative information on the relative coverage of surfacial C−Si bonds for the various alkylated surfaces. This peak is useful for providing an estimate of the alkyl coverage because, unlike the infrared spectra in the C−H stretching region, interpretation of the intensity of this low-energy C1s peak is not confounded by the presence of adventitious hydrocarbons on the Si surface.[51,52,58,59] The peak-area ratio of the C−Si peak to the Si2p signal (C−Si/Si2p) of each alkyl group was measured relative to the C−Si/Si2p peak-area ratio for the CH_3-terminated Si(111) surface (Table 1). $Si-CH=CH-CH_3$ surfaces showed a C−Si/Si2p ratio of 110 ± 10% relative to that of the CH_3-Si surface, indicating that the $Si-CH=CH-CH_3$ can be packed at a very high density by this two-step alkylation method. The XPS peak-area analysis shows that the stoichiometric ratio between the C atom bonded directly to the Si (at 284.0 eV) and to the two C atoms bonded far away from the Si surface (at 285.2 eV) is 1:2, indicating that these XPS peaks are due to $Si-CH=CH-CH_3$ molecules. Similarly, the C−Si/Si2p peak-area ratios for $Si-C\equiv C-CH_3$ and $Si-CH_2-CH_2-CH_3$ were 105 ± 05% and 50 ± 10%, respectively, relative to that of CH_3-Si surface.[57−60,62]

(62) Hunger, R.; Fritsche, R.; Jaeckel, B.; Jaegermann, W.; Webb, L. J.; Lewis, N. S. *Phys. Rev. B* **2005**, *72*, 045317–7.

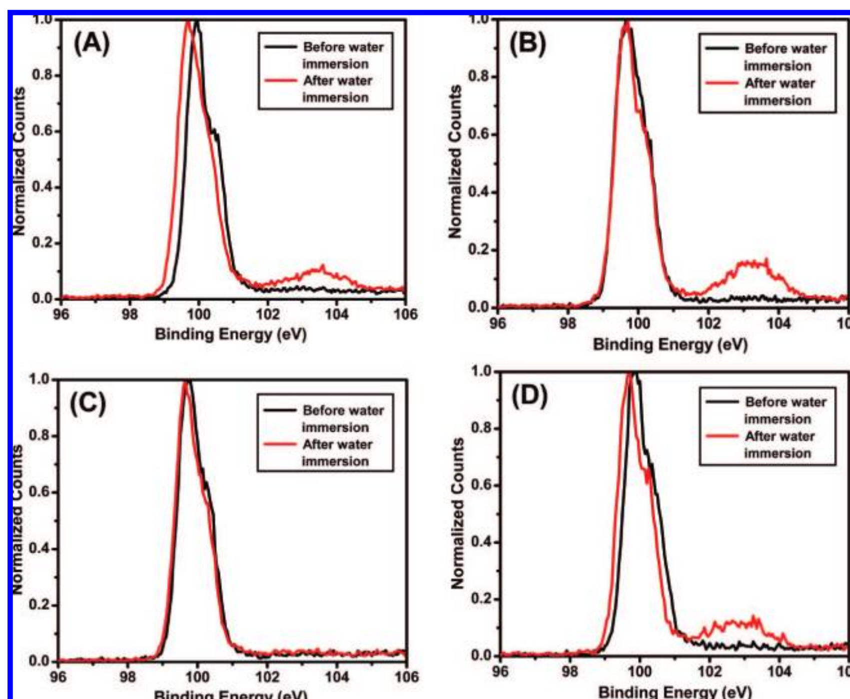

Figure 3. XPS spectra of the Si2p region of (A) Si−CH_3, (B) Si−CH_2−CH_2−CH_3, (C) Si−CH═CH−CH_3, and (D) Si−C≡C−CH_3 before and after immersion in water at room temperature.

Several studies have shown that well-ordered monolayers on silicon prevent the oxidation of silicon to silicon dioxide while disordered monolayers are less suitable to do so.[5,63,64] Thus, the absence of oxidized silicon is further proof that the monolayers are well-ordered. Silicon wafers readily oxidize to yield a thin layer of silicon dioxide on the surface, but well-ordered alkyl monolayers greatly inhibit the rate of this oxidation.[5,27,63−65] Thus, by measuring the XPS as a function of time, we can learn how well the monolayers protect silicon from oxidation.

Figures 1 and 2 show the evolution of the XPS spectra of molecularly modified Si surfaces as a function of time exposed to ambient air. Oxidation of the Si surface was monitored by the growth of the broad Si_x^+ peak between 101.0 and 105.0 eV. Relative to H-terminated Si, Si−CH═CH−CH_3 surfaces exposed to air over a period of more than two months in the dark showed greatly reduced surface oxidation (Part B of Figure 1 and Figure 2).[52,58] Because oxidation involves the presence of water at the surface, it may be concluded that the dense hydrophobic layer prevents the penetration of water through the monolayer. This result is significant because adventitious oxidation degrades the electronic properties of the Si surface.[40,66,67] The surface oxidation for the other molecularly modified Si surfaces is shown in parts A and C of Figure 1 and in Figure 2. The Si−C≡C−CH_3 surface showed no oxidation up to 25 days (part C of Figure 1 and Figure 2). Yet, beyond that period, the oxidation rate increased with time. The Si−CH_2−CH_2−CH_3 surface showed more oxidation than Si−CH═CH−CH_3, Si−C≡C−CH_3, and Si−CH_3, mostly due to its lower surface coverage (∼50% as compared with ∼100% surface coverage of the other molecules).[52,57−59]

Stability of monolayers on Si surfaces is one of the main aspects that needs to be investigated for applications. The stability of Si in water is particularly important for potential applications in DNA sensing, biosensors, surfaces for growth of biological cells, and, also, molecular electronics.[51,63−65] To study the quality of monolayers, we investigated their stability in water, chloroform, and hexane. We immersed the samples in water, chloroform, or hexane for 24 h at room temperature and then dried and characterized them by XPS. If the monolayer is well-ordered and stable, we expect that the XPS spectrum will not show the presence of SiO_2, and vice versa.[5,63] The XPS results did not show any SiO_2 peak for the Si−CH═CH−CH_3 surface after water immersion (part C of Figure 3). However, prominent peaks of SiO_2 were observed after immersion of Si−CH_3 (part A of Figure 3), Si−CH_2−CH_2−CH_3 (part B of Figure 3), and Si−C≡C−CH_3 surfaces (part D of Figure 3) in water. There were no SiO_2 peaks observed for the Si−C≡C−CH_3, Si−CH═CH−CH_3, and Si−CH_3 surfaces after chloroform and hexane immersion (Figure 4). However, a peak of SiO_2 was observed for the Si−CH_2−CH_2−CH_3 surface, mostly due to the 50% coverage of the monolayer. The constant C−Si/Si2p ratio for the Si−CH═CH−CH_3 surface in XPS before and after exposure to water indicated that the layer was not removed. These results provide further evidence that stable Si−CH═CH−CH_3 monolayers were formed and that they are stable under a range of conditions, if compared to Si−C≡C−CH_3, Si−CH_2−CH_2−CH_3, and Si−CH_3 monolayers, thus widening the range of potential applications.

3.2. Spectroscopic Ellipsometry Analysis. The analysis of the spectroscopic ellipsometry confirms the attachment of the studied organic molecules from Grignard reagents. The thickness extracted from the spectra depends on the nature of the

(63) Sieval, A. B.; Linke, R.; Zuilhof, H.; Sudhölter, E. J. R. *Adv. Mater.* **2000**, *12*, 1457–1460.
(64) Arafat, S. N.; Dutta, S.; Perring, M.; Mitchell, M.; Kenis, P. J. A.; Bowden, N. B. *Chem. Commun.* **2005**, *25*, 3198–3200.
(65) Perring, M.; Dutta, S.; Arafat, S. N.; Mitchell, M.; Kenis, P. J. A.; Bowden, N. B. *Langmuir* **2005**, *21*, 10537–10544.
(66) Yablonovitch, E.; Allara, D. L.; Chang, C. C.; Gmitter, T.; Bright, T. B. *Phys. Rev. Lett.* **1986**, *57*, 249–252.
(67) Stutzmann, M.; Garrido, J. A.; Eickhoff, M.; Brandt, M. S. *Phys. Status Solidi A* **2006**, *203* (14), 3424–3437.

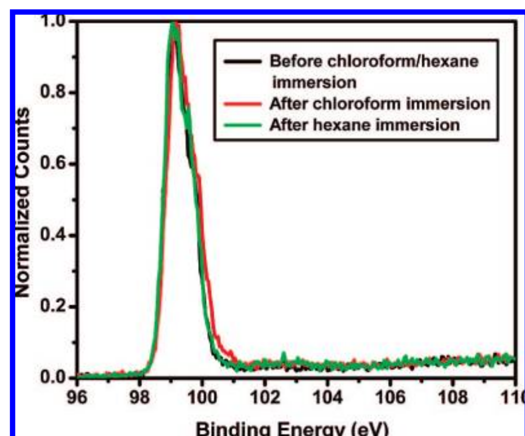

Figure 4. XPS spectra of the Si2p region of Si−CH═CH−CH$_3$ surfaces before and after immersion in chloroform or hexane for 24 h at room temperature.

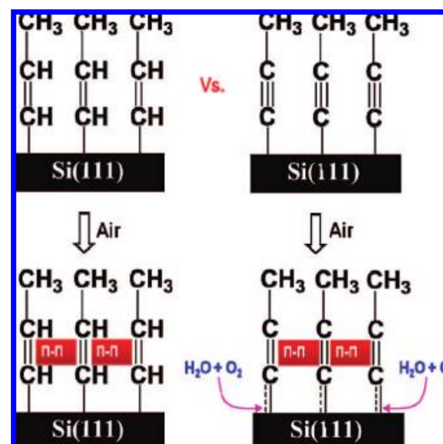

Figure 5. Schematic illustration of the oxidation mechanism for the Si−CH═CH−CH$_3$ and Si−C≡C−CH$_3$ molecules.

Table 2. Normalized Peak Intensities in ToF-SIMS Spectra of the Molecularly Modified Si(111) Surfaces

	type of molecular termination			
ToF SIMS signal	Si−CH$_3$	Si−CH$_2$−CH$_2$−CH$_3$	Si−CH═CH−CH$_3$	Si−C≡C−CH$_3$
$SiC_xH_y^+$ Peak Intensities in Positive ToF-SIMS Spectra				
$SiCH_3^+$	63104	1127370	337621	356237
$SiC_3H_7^+$	3016	87545	30779	9658
$SiC_3H_5^+$	2403	2579	29598	10399
$SiC_3H_3^+$	10	7100	37961	189382
SiO_2 and $C_xH_y^-$ Peak Intensities in Negative ToF-SIMS Spectra				
SiO_2	1841	11606	2033	12809
CH_3^-	261	776	162	306
$C_3H_7^-$	8	700	13	7
$C_3H_5^-$	25	26	52	45
$C_3H_3^-$	227	270	715	34366

molecule's length. Average thicknesses of about 2.6, 4.2, 5.3, and 5.8 Å were obtained for Si−CH$_3$, Si−CH$_2$−CH$_2$−CH$_3$, Si−CH═CH−CH$_3$, and Si−C≡C−CH$_3$, respectively. These results were found in a good agreement with the theoretical lengths obtained by our DFT calculations (section 2.5): 2.3 Å for Si−CH$_3$, 4.4 Å for Si−CH$_2$−CH$_2$−CH$_3$, 5.0 Å for Si−CH═CH−CH$_3$, and 5.8 Å for Si−C≡C−CH$_3$. These findings suggest that the molecules are packed vertically and normal to the surface.

3.3. ToF-SIMS analysis. Table 2 summarizes the main normalized $SiC_xH_y^+$ and $C_xH_y^-$ peak intensities in positive and negative ToF-SIMS spectra of the molecularly modified Si(111) surfaces. ToF-SIMS spectra of alkylated Si(111) generally contain a number of hydrocarbon ($C_xH_y^-$) and silicon−hydrocarbon ($SiC_xH_y^+$) fragments. The presence of $SiC_xH_y^+$- and $C_xH_y^-$-type fragments suggests covalent bonding of alkyl chains to the silicon surfaces through Si−C bonds. For Si−C≡C−CH$_3$ surfaces, the $SiC_3H_3^+$ cations are more easily produced, suggesting an easily sputtering-induced decomposition of the near surface region by ToF-SIMS. This observation is found in agreement with the literature findings, where $SiC_xH_y^+$ cations were produced more easily from monolayers with less densely packed alkyl chains.[41,42,68] For the same surfaces, the observation of more $C_3H_3^-$ anions and more SiO_2 signals from the negative ToF-SIMS spectra provides an additional evidence for the surface oxidation in air. For the Si−CH═CH−CH$_3$ surfaces, the observation of hardly sputtered $C_3H_5^-$ anions and a lower amount of SiO_2 (as compared to Si−C≡C−CH$_3$ surfaces) indicate that these monolayers are densely packed and more robust. When compared to other molecules (characterized by $C_3H_3^-$ vs $C_3H_7^-$ vs CH_3^-), Si−CH═CH−CH$_3$ produced less $C_3H_5^-$ anions and less SiO_2 after sputtering, indicating superior stability.

The presence of a small amount of SiO_2 on Si−CH═CH−CH$_3$ after extremely long exposure to air and also after extensive immersion in polar and nonpolar solvents could be attributed to the $\pi-\pi$ interaction between the molecules.[69] In the case of Si−C≡C−CH$_3$ surfaces, $\pi-\pi$ interactions occur between the adjacent molecules but leave one pair of electrons free (Figure 5). This pair of free electrons might easily transfer to the atop Si site (beneath the molecule) and interact with oxidizing agents (e.g., water, O_2, etc.).[5,63,64,70] The ToF-SIMS results (Table 2) indicate that direct interaction between the free electron pair and oxidizing agent is possible too, mostly for ca. 10% of the molecules on the surface. In the case of Si−CH$_2$−CH$_2$−CH$_3$ surfaces, neither full (100%) coverage nor $\pi-\pi$ interactions exist, thus explaining their low resistance to oxidation processes. On the basis of these findings, Si−CH═CH−CH$_3$ monolayers can provide better stability than those of the other molecules without the interfacial silicon oxide while eliminating interfacial trap states.

3.4. Subsequent Functionalization of Propenyl-Terminated Surfaces. In previous work, further functionalization of octadecyl monolayers was addressed using a two-step process: the octadecyl monolayer was first chlorosulfonated by a photo-initiated free radical reaction, and this step was followed by sulfonamide formation via reaction of the sulfonyl chloride with an amine.[71] Through the use of this approach, it was possible to functionalize octadecyl monolayers on Si surfaces with a diverse range of amines, including those containing DNA and dendrimers,[61] and also to react octadecyl monolayers with singlet carbenes.[61] These studies represent an important advance in the ability to design and control the chemical properties of surfaces by further functionalization of Si−CH═CH−CH$_3$.

(68) Lua, Y.-Y.; Niederhauser, T. L.; Matheson, R.; Bristol, C.; Mowat, I. A.; Asplund, M. C.; Linford, M. R. *Langmuir* **2002**, *18*, 4840–4846.

(69) Nam, H.; Granier, M.; Boury, B.; Park, S. Y. *Langmuir* **2006**, *22*, 7132–7134.

(70) Kung, H.; Wu, S. M.; Wu, Y-J; Yang, Y. W; Chiang, C. M. *J. Am. Chem. Soc.* **2008**, *130*, 10263–10273.

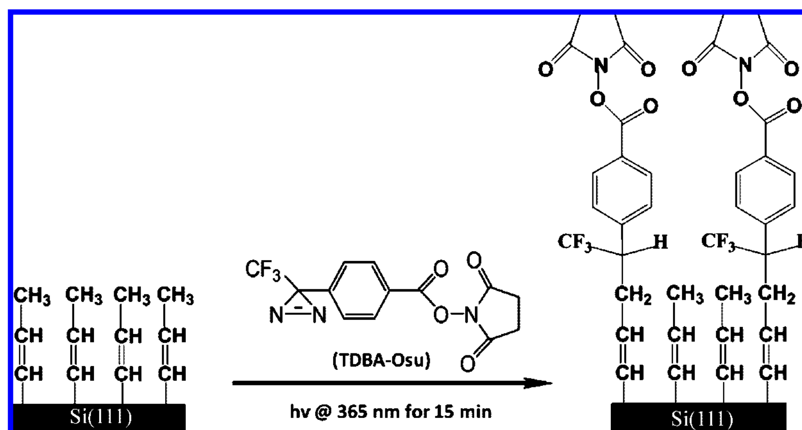

Figure 6. Schematic illustration of the secondary functionalization of the Si−CH═CH−CH_3 with photoactive aryldiazirine cross-linker (TDBA-OSu).

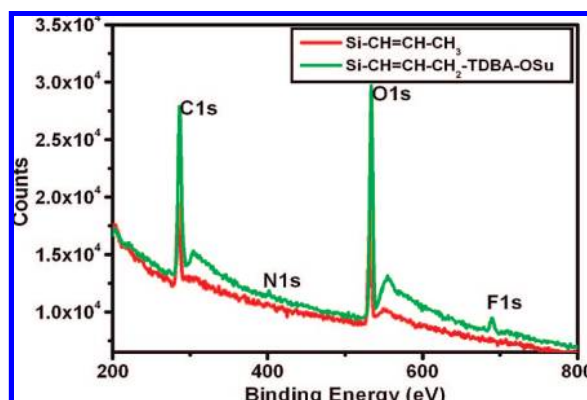

Figure 7. XPS wide-scan data for a propenyl surface before and after functionalization with TDBA-OSu.

Figure 6 gives an overview of the secondary functionalization used to covalently modify the methyl groups of the studied propenyl monolayer. In this approach, TDBA-OSu (a commercially available photoactive aryldiazirine cross-linker) was used as the key compound. This functionality inserts into the carbon−hydrogen bonds of the terminal methyl groups through a highly reactive singlet-state carbene intermediate at one end and leaves reactive amino groups at other end.[61] The wide-scan XPS spectra for (Si−CH═CH−CH_3)- and (Si−CH═CH−CH_2−TDBA-OSu)-terminated surfaces are shown in Figure 7. After attachment of TDBA-OSu on Si−CH═CH−CH_3, the F1s peak appears around 680.0 eV due to the trifluoromethyl group of the TDBA-OSu cross-linker. The small N1s peak is also visible in the XPS survey spectrum at 402.4 eV due to the low atomic ratio of nitrogen in TDBA-OSu. Overall, these results show that the TDBA-OSu is covalently attached to the Si−CH═CH−CH_3 surface.

The C1s signal of the (Si−CH═CH−CH_2−TDBA-OSu)-terminated surface can be deconvoluted into four peaks (part A of Figure 8), from low to high binding energy, as follows: (i) a peak at 284.0 eV for the emission from core-level electrons of carbon atoms that are covalently bonded to the relatively electropositive silicon (C−Si); (ii) a peak at 285.1 eV for carbons in the aliphatic hydrocarbon chain; (iii) a peak at 286.8 eV for α-carbons adjacent to the carbonyl carbon atoms (these three α-carbons shift much more than an ordinary α-CH_2 in an alkyl chain because of the strong electron-withdrawing effect from the imide group in the TDBA-OSu moiety[72,73]); and (iv) a peak at 289.6 eV for the carbonyl carbon atoms. The ratio between these four peaks for a 100% (Si−CH═CH−CH_2−TDBA-OSu)-terminated surface was 1.5:8.9:1.5:1.0, which can be compared to the theoretical ratio of 1:8:3:3. On the basis of these ratios, it is possible to see that this method generates ca. 50% density of reactive amino groups on the surface.

The C−Si/Si2p ratio of the (Si−CH═CH−CH_2−TDBA-OSu)-terminated surface (105 ± 5%) was similar to that of the (Si−CH═CH−CH_3)-terminated one (110 ± 10%), indicating that the propenyl monolayer was not damaged during the secondary functionalization with TDBA-OSu. On the other hand, at the end of the secondary functionalization process, a small amount of oxide, equivalent to 5% of a monolayer, was observed (part B of Figure 8). The small ratio of the SiOx and Si2p peak areas in the Si−CH═CH−CH_2−TDBA-OSu sample could be attributed to a typical accompanying effect of the UV exposure during the functionalization process (cf. refs 61 and 72). The oxide evolution of the (Si−CH═CH−CH_2−TDBA-OSu)-terminated surface upon exposure to ambient air (not shown) revealed stability similar to that for Si−CH═CH−CH_3 shown in Figure 2 (excluding a shift of ~5% in the *y* axis, which stands for the SiOx/Si2p peak-area ratio). This finding indicates that the (5% monolayer of) oxide evolved during the functionalization process has no degradation effects on the stability of the Si−CH═CH−CH_2−TDBA-OSu)-terminated surfaces.

4. Summary and Conclusions

Alkylation of Si(111) surfaces with CH_3−CH═CH−MgBr through a two-step chlorination/alkylation procedure gives nearly 100% coverage, with a double-bonded molecule attached to nearly every silicon atop atom on an unreconstructed Si(111) surface using a Si−C bond. We compared the properties of the Si−CH═CH−CH_3 surface with Si−C≡C−CH_3, Si−CH_2−CH_2−CH_3, and Si−CH_3 surfaces. Si−CH═CH−CH_3 surfaces showed excellent surface passivation, with a very small amount of silicon oxide formed after more than two months of exposure to air when compared to Si−C≡C−CH_3,

(71) Cicero, R.; Wagner, P.; Linford, M. R.; Hawker, C. J.; Waymouth, R. M.; Chidsey, C. E. D. *Polym. Prepr. (Am. Chem. Soc., Div. Polym. Chem.)* **1997**, *38*, 904–905.

(72) Yang, M.; Teeuwen, R. L. M.; Giesbers, M.; Baggerman, J.; Arafat, A.; Wolf, F. A. D.; Hest, J. C. M. V; Zuilhof, H. *Langmuir* **2008**, *24*, 7931–7938.

(73) *Surface Analysis by Auger and X-ray Photoelectron Spectroscopy*; Briggs, D., Grant, J. T., Eds.; IM Publications: Chichester, U.K., 2003.

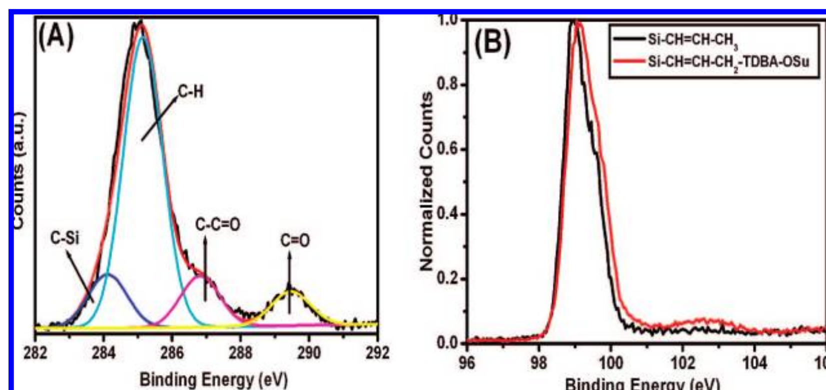

Figure 8. (A) XPS scans of C1s segment, and (B) Si2p region of propenyl surface before and after functionalization with TDBA-OSu.

$Si-CH_2-CH_2-CH_3$, and $Si-CH_3$ surfaces. Our results also indicate that the $Si-CH=CH-CH_3$ surface is more stable against the different polar and nonpolar solvent attacks when compared to $Si-C\equiv C-CH_3$, $Si-CH_2-CH_2-CH_3$, and $Si-CH_3$ surfaces. Finally, the attachment of a TDBA-OSu cross-linker on propenyl-terminated Si(111) has been demonstrated. The $Si-CH=CH-CH_2-$TDBA-OSu surface has been terminated with amino-reactive *N*-succinimidyl groups, which are used to immobilize the different molecules in the next layer. The advantage of this approach is that having a better-defined monolayer provides the possibility of controlling the density of reactive cross-linkers that are covalently bound on top of the monolayer and increasing their accessibility to, for example, the binding pockets of specific sites in biomolecules.[10,61,71,72] Additionally, this approach offers an avenue for introducing well-defined molecular wires between Si surfaces and micro- or macrocontacts[74,75] as well as for fabrication of hybrid organic−silicon molecular or optical devices.[46−48] To this end, this approach has a high potential in preserving the stability of the molecularly modified surfaces/junctions and in preventing (or reducing) the interdiffusion of contacting metals into the monolayer and/or the Si substrate.[74,75] Finally, it can be expected that the ability to control the average distance between the termination groups added by subsequent functionalization of, for example, $Si-CH=CH-CH_3$ will have a significant impact on the future molecular electronic, sensing, and biochip technologies. Control of the distance between the functional groups is of great interest because it offers a unique avenue for studying the electrostatic effects of ideal and nonideal polar organic monolayers and their implications for electronic devices.[76]

Acknowledgment. The authors acknowledge the Marie Curie Excellence Grant of the FP6, the US-Israel Binational Science Foundation (BSF), and the Russell Berrie Nanotechnology Institute for financial support. H.H. holds the Horev Chair for the Leaders in Science and Technology.

JA804674Z

(74) Haick, H.; Cahen, D. *Prog. Surf. Sci.* **2008**, *83*, 217–261.
(75) Haick, H.; Cahen, D. *Acc. Chem. Res.* **2008**, *41*, 359–366.
(76) Natan, A.; Kronik, L.; Haick, H.; Tung, R. T. *Adv. Mater.* **2007**, *19*, 4103–4117.